Insights into the iron and sulfur energetic metabolism of *Acidithiobacillus ferrooxidans* by microarray transcriptome profiling

Raquel Quatrini [a,1], Corinne Appia-Ayme [b,1], Yann Denis [b], Jeanine Ratouchniak [b], Felipe Veloso [a], Jorge Valdes [a], Claudia Lefimil [e], Simon Silver [c], Frank Roberto [d], Omar Orellana [e], François Denizot [b], Eugenia Jedlicki [e], David Holmes [a], Violaine Bonnefoy [b,*]

[a] *Andrés Bello University and Millennium Institute for Fundamental and Applied Biology, Santiago, Chile*
[b] *Laboratoire de Chimie Bactérienne, IBSM, CNRS, Marseille, France*
[c] *University of Illinois, Chicago, USA*
[d] *Idaho National Engineering and Environmental Laboratory, Idaho Falls, USA*
[e] *I.C.B.M., Faculty of Medicine, University of Chile, Santiago, Chile*

Abstract

Acidithiobacillus ferrooxidans is a well known acidophilic, chemolithoautotrophic, Gram negative, bacterium involved in bioleaching and acid mine drainage. In aerobic conditions, it gains energy mainly from the oxidation of ferrous iron and/or reduced sulfur compounds present in ores. After initial oxidation of the substrate, electrons from ferrous iron or sulfur enter respiratory chains and are transported through several redox proteins to oxygen. However, the oxidation of ferrous iron and reduced sulfur compounds has also to provide electrons for the reduction of NAD(P) that is subsequently required for many metabolic processes including CO_2 fixation. To help unravel the enzymatic pathways and the electron transfer chains involved in these processes, a genome-wide microarray transcript profiling analysis was carried out. Oligonucleotides corresponding to approximately 3000 genes of the *A. ferrooxidans* type strain ATCC23270 were spotted onto glass-slides and hybridized with cDNA retrotranscribed from RNA extracted from ferrous iron and sulfur grown cells. The genes which are preferentially transcribed in ferrous iron conditions and those preferentially transcribed in sulfur conditions were analyzed. The expression of a substantial number of these genes has been validated by real-time PCR, Northern blot hybridization and/or immunodetection analysis.

Our results support and extend certain models of iron and sulfur oxidation and highlight previous observations regarding the possible presence of alternate electron pathways. Our findings also suggest ways in which iron and sulfur oxidation may be co-ordinately regulated. An accompanying paper (Appia-Ayme et al.) describes results pertaining to other metabolic functions.

Keywords: Iron oxidation; Sulfur oxidation; Microarray analysis; Extremophile; Electron transport; Bioinformatics

1. Introduction

Acidithiobacillus ferrooxidans is one of the most studied microorganism commonly found in acid mine drainage (see references in [1,2]). One can wonder at how life is possible in such extreme environments (high proton

* Corresponding author.
E-mail addresses: rquatrini@yahoo.com.ar (R. Quatrini), cappiaayme@yahoo.fr (C. Appia-Ayme), ejedlick@med.uchile.cl (E. Jedlicki), dsholmes2000@yahoo.com (D. Holmes), bonnefoy@ibsm.cnrs-mrs.fr (V. Bonnefoy).
[1] These authors contributed equally to the work.

and metal concentration). In fact, *A. ferrooxidans* takes advantage of these conditions and gains energy required for growth from the aerobic oxidation of ferrous iron (FeII) and reduced sulfur compounds to ferric iron (FeIII) and sulfuric acid, respectively. The oxidation products then attack chemically the metal sulfides [3] leading to metal solubilization and ore desulfurization. Therefore, elucidating the unusual energetic metabolism of *A. ferrooxidans* is of central importance to understanding its bioleaching and bioremediation properties. Consequently, understanding the respiration of iron and reduced sulfur compounds is of wide interest, not only scientifically, but also from an economic and environmental point of view.

Iron-based energetic metabolism has been studied for several years leading to the proposal of a number of respiratory chain models [4–9]. The currently accepted model [9] is based on genetic [9,10] and biochemical evidence [11,12], and is further supported by the subcellular localization of the proposed redox partners [13,14]. On the other hand, the study of the energetic metabolism of reduced sulfur compounds is more complicated than for iron, because (i) it involves several enzymatic reactions, (ii) only some of them are coupled to the respiratory chain(s) and (iii) these couplings occur at different points of the respiratory chain(s). While several enzymes proposed to be involved in sulfur dissimilation have been known for a long time [15–21], it is only recently that some results were reported on the sulfur respiratory chains [22,23]. To add to the complexity of *A. ferrooxidans* energetic metabolism, the oxidation of ferrous iron and of reduced sulfur compounds has to provide electrons for the reduction of NAD(P) that is subsequently required for many metabolic processes, such as carbon and nitrogen fixation. It is now clear that *A. ferrooxidans* respiratory chains to oxygen are redundant and branched [22]. Furthermore, from the *A. ferrooxidans* genome sequence analysis, the existence of several electron transfer proteins has been inferred [13,22,24], but the respiratory chain to which they belong was not known for most of them.

Despite considerable effort, *A. ferrooxidans* remains largely recalcitrant to standard genetic techniques for its manipulation, although promising progress has been made for developing a conjugation system for genetic exchange with *Escherichia coli* [25,26]. Such deficiency seriously impedes the direct experimental investigation of the metabolism of *A. ferrooxidans* and gene knockouts are still difficult to obtain. Nevertheless, the study and comparison of gene expression profiles is an alternative that can circumvent this limitation. Recently, the *A. ferrooxidans* genome sequence has been made available by The Institute for Genomic Research. As part of the growing effort to understand *A. ferrooxidans* physiology its genome has been annotated and curated (Holmes et al., 2005, manuscript in preparation), making feasible genome-wide comprehensive studies through the construction and use of microarray technology.

To gain further insight into the physiological role of the known redox proteins and to help identify yet unknown or missing components involved in iron and sulfur respiratory chains to oxygen, we have undertaken a global transcriptomic approach. In the present work, we have compared the expression profiles of the *A. ferrooxidans* cells grown on iron with those grown on sulfur, focusing our interpretations on the energy metabolism functions.

2. Materials and methods

2.1. Strain and culture conditions

A. ferrooxidans ATCC 23270 was obtained from the American Type Culture Collection. *A. ferrooxidans* was grown at 30 °C under oxic conditions (200 rpm) in (i) FeII-medium consisting of 62 mM $FeSO_4$–$7H_2O$ in 9 K basal salts solution ($(NH_4)_2SO_4$: 0.4 g/l; K_2HPO_4: 0.4 g/l; $MgSO_4$–$7H_2O$: 0.4 g/l adjusted to pH 1.6 with H_2SO_4; (ii) S^0-medium consisting of 1% (w/v) elemental sulfur in 9 K basal salts solution ($(NH_4)_2SO_4$: 0.4 g/l; K_2HPO_4: 0.4 g/l; $MgSO_4$–$7H_2O$ adjusted to pH 3.5 with H_2SO_4.

2.2. Materials

The TRIZOL® reagent was from Invitrogen. The High Pure RNA isolation kit was from Roche Applied Biosystem. The 50-mer oligonucleotides were synthesized, and HPCR® (High Purity Salt Free) purified by MWG Biotech. The size of randomly chosen oligonucleotides was controled by MALDI-TOF mass spectroscopy by MWG Biotech. The slides (UltraGAPS), the spotting buffer (Pronto!™ Universal Printing Kit), the labelling and clean-up reagents (ChipShot™ Labelling Clean-Up System) and the pre-hybridization and hybridization reagents (Pronto!™ Microarray Reagent System) were from Promega-Corning (Pronto!™ *Plus* System). Cy®3 and Cy®5-labeled nucleotides were from Amersham Biosciences. LightCycler Fast Start DNA master (plus) SYBR Green I PCR kit was from Roche Applied Biosystems.

2.3. Oligonucleotide design

For each of the 3037 putative ORFs predicted in the genomic sequence of *A. ferrooxidans* ATCC 23270 (TIGR release September 2003; 2.98 Mb), an internal 50-mer oligonucleotide was designed using the Oligoarray

software (Version 1.0). Oligonucleotide design considerations include narrow melting temperature (92 ± 7 °C), and avoidance of self-annealing structures. To exclude redundant oligonucleotides and minimize cross-hybridization, a Blast search (using e^{-10} as cutoff) was carried out. A special set of control oligonucleotides (negative, positive, tiled and antisense sequences) was included to evaluate probe specificity and adjust the hybridization conditions. 50-mer oligonucleotides corresponding to the CDS of the *gfp* gene from *Aequorea* sp., the *rad9* gene form *Saccharomyces cereviciae* and the *idi2* gene from human were used as negative controls.

Unmodified 50-mer oligonucleotides have been shown to enable high signal intensity and high specificity [27]. Therefore, unmodified oligonucleotides, synthesized by MWG Biotech at a 10 nm scale and at 100 μM were used.

2.4. Oligonucleotides spotting

The unmodified 50-mer oligonucleotides were diluted to 50 μM in Corning Pronto!™ Universal Spotting Solution for spotting purposes. They were spotted in duplicate on Corning UltraGAPS slides, coated with Gamma Amino Propyl Silane, with an 8 pin Affimetrix 427 Arrayer at the Marseille-Nice Genopole (France). They were subsequently immobilized by UV cross-linking with the UV Stratalinker 2400 (Stratagene) and stored in a dessicator cabinet until use.

2.5. RNA preparation

A. ferrooxidans mid logarithmic cultures grown in the presence of FeII (62 mM $FeSO_4$) or S^0 (0.5% S^0) as energy source (30 °C, 200 rpm) were harvested by centrifugation at 4 °C and immediately processed for RNA extraction. Cells were washed in 9 K buffer (pH adjusted) to remove iron traces or sulfur particles before further treatment. Total RNA was extracted using a modified acid–phenol extraction method [28], including a preliminary TRIZOL® reagent (Invitrogen) extraction step. This RNA was used directly for cDNA synthesis and labelling. For real-time PCR, RNAs were additionally purified with the High Pure RNA isolation kit (Roche Applied Biosystem) and treated twice with DNAse I (Roche Applied Biosystem). The lack of DNA contamination was checked by PCR on each RNA sample.

2.6. Labelled cDNA synthesis and hybridization

The ChipShot™ Labelling Clean-Up System (Promega-Corning) was used to generate fluorescently labeled cDNA via direct incorporation of Cy®3 and Cy®5-labeled nucleotides from Amersham Biosciences. The reverse transcription reaction was performed in the presence of 5 μg total RNA and random hexamers (Protocols: www.promega.com). Two independent cDNA preparations were labeled once with each dye (reverse dye labeling) to account for sampling differences, biases in dye coupling or emission efficiency of Cy®-dyes. Labelled cDNA was purified from contaminating fluorescent dNTPs and degraded RNA using the ChipShot Labelling Clean-Up System (Promega-Corning). Dye incorporation efficiency was determined by absorbance readings at 260, 550 and 650 nm and the frequency of incorporation (FOI, pmol of dye incorporated per ng of cDNA) was calculated according to Promega's instructions. Optimally labelled samples were combined, vacuum-dried and resuspended to a final volume of 40–50 μL in Corning Pronto! Universal Hybridization Buffer.

The Pronto !™ Universal Hybridization kit was used according to Promega's instructions. Briefly, the combined denatured target cDNA samples (95 °C for 5 min) were hybridized to the spotted slides for 14 h at 42 °C in the Corning hybridization chamber. Following hybridization, slides were washed in serial dilutions of Corning Wash Buffers as recommended by the manufacturer and dried by centrifugation at 1200×*g* for 2 min.

2.7. Image acquisition and data analysis

Microarrays were scanned for the Cy®3 and Cy®5 fluorescent signals using the ScanArray 4000 Microarray Analysis System (PerkinElmer Life Sciences, Inc.) at a resolution of 10 μm per pixel. Scanning parameters (laser power: 85–95 and photomultiplier voltage: 90–95) were adjusted so that overall intensities in both fluorescent channels were balanced and few spots were saturated (to maximize the dynamic range). Scans stored as 16-bit TIFF (Tagged Information File Format) image files and then analyzed with the image quantification software package GenePix Pro 4.0 (Axon Instruments, Inc.). Addressing information, raw signal intensity readings and quality parameters for each spot were recorded. Low-quality spots (spots smaller than 60 μm or bigger than 160 μm in diameter, sub-circular in shape and/or exhibiting uneven fluorescence distribution) were flagged and filtered out. Genes with median signal intensities less than two standard deviations above background in both channels were considered as not detected and array elements that approached the maximum value (65.535 per pixel for a 16-bit scanner) were considered as saturated and excluded from further

statistical analysis. Local background was subtracted from the recorded spot intensities (median values). Negative values (i.e. local background intensities higher than spot signal) were considered as no data. Median spot intensities were Log transformed (Log2) and normalized to account for any difference in total intensity between the scanned images due to pin effects (Pin group location normalization), dye and slide effects (Scale normalization) and intensity-dependent effects (Lowees normalization) using the R package (Version 1.8.1; URL http://www.R-project.org.). The processed FeII and S^0 signal intensities for each spot were used for calculating the expression ratio FeII/S^0. Eight ratio values per gene, resulting from direct and reverse labelling and replicate experiments, were used for further statistical analysis of the data. The statistical significance of differential expression in FeII or S^0 grown cells, was assessed using R package applying to the data set, the Student *t*-test [28].

2.8. Real-time PCR

The relative abundances of a set of differentially expressed genes and a set of invariant genes, according to the microarray results obtained, were determined in FeII- and S^0-grown cells by real-time PCR. Specific primers for the genes of interest amplifying average products of 300 bp with about 50 GC % and about 55 °C Tm were designed. Equal amounts of *A. ferrooxidans* DNAseI-treated total RNA were retro-transcribed from these primers with the Superscript II™ RNase H^- (InVitro Life Technologies) at 42 °C for 50 min, and then treated at 70 °C for 15 min to inactivate the enzyme. The real-time PCR quantifications were realized at the transcriptome platform of the I.B.S.M. (Marseille, France) on the total cDNA obtained, using the LightCycler instrument and the LightCycler Fast Start DNA master (plus) SYBR Green I PCR kit (Roche Applied Biosystems) with external standards as described in Roche Molecular Biochemicals technical note no. LC 11/2000. The real-time PCR experiments were performed twice, with both independent total RNA and cDNA preparations by the comparative threshold cycle method. The calculated threshold cycle (Ct) for each gene was normalized to Ct of the *rrs* gene, coding for the 16S rRNA which expression is invariant under FeII- and S^0-growth conditions [10].

3. Results and discussion

3.1. A. ferrooxidans microarrays analysis

The genomic expression profiles of *A. ferrooxidans* ATCC 23270 growing on FeII or S^0 media were determined and compared with one another. To identify the genes differentially affected by the energy source, the following statistical criteria were employed: (i) genes with *P* values >0.01 were considered as not regulated regardless of their differential expression level; (ii) genes with a *P* value of <0.01 were considered to have significant differential expression and thus regarded as up-regulated either in FeII or in S^0

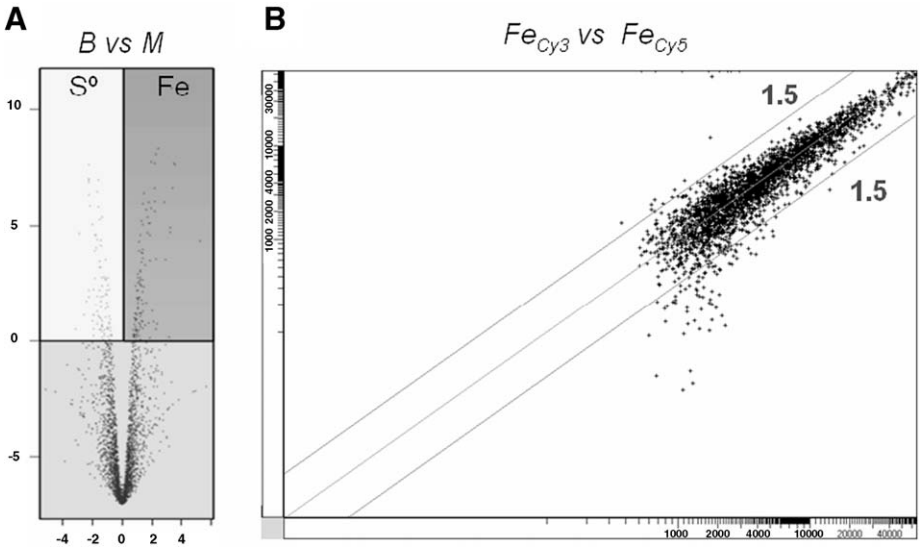

Fig. 1. Differentially expressed genes in *A. ferrooxidans* microarrays. (A) Odds of being differentially expressed [*B*-statistic versus *M* (Log2 ratio FeII/S^0)]. (B) Fold-change cut-off determination by hybridization of identical cDNA samples labelled with Cy®3 and Cy®5.

conditions (Fig. 1A). The fold-change cut-off to be used for the identification of the genes exhibiting differential expression between treatments was assessed by hybridization of identical cDNA samples (total RNA extracted from FeII-grown cells) labeled with Cy®3 or Cy®5 dyes. The pattern of hybridization revealed a linear correlation of the data and a fold change in gene expression level (*M*: Log2 ratio FeII/S^0) no larger that 1.5 (Fig. 1B). Similar cut-off values have been reported as being biologically significant elsewhere. Therefore, genes with a positive Log2 FeII/S^0 ratio (*M*) were considered to be more expressed in FeII- than in S^0 and vice-versa, while the genes with a Log2 FeII/S^0 ratio (*M*) close to zero were considered to be similarly expressed in both conditions.

On the basis of the criteria described above, the expression level of more than 200 genes of *A. ferrooxidans* was affected by the presence of either FeII or S^0 as energy source in the growth media (Fig. 2). The comparison of the transcriptional profiles of FeII-grown cells versus S^0-grown cell indicated that about 120 genes were induced (Max = up to 38 fold) in FeII conditions and about 90 were specifically induced (Max = up to 10 fold) in S^0 conditions.

3.2. Energy source (FeII or S^0) expression profile

The genes expressed differentially according to the energy source can be divided into seven functional categories: energy metabolism, central intermediary metabolism, regulatory functions, protein translation, amino acid biosynthesis, cell wall and envelope constituents, and miscellaneous (unknown function). In this paper, we will analyze the genes encoding proteins involved in the energetic metabolism while results pertaining to the other metabolic functions, and more particularly to the carbon metabolism, are described in the accompanying paper (Appia-Ayme et al.).

Table 1 summarizes the data obtained on genes encoding electron transfer proteins we have previously suggested to be involved in FeII or S^0 energetic metabolism ([9,22,30,31], Bruscella, Appia-Ayme, Levican, Ratouchniak, Holmes, Jedlicki and Bonnefoy, manuscript in preparation).

3.2.1. Characterization of FeII-induced genes encoding electron transporters

In FeII conditions, the *petI* operon encoding one of the bc_1 complexes ([24,30,31], Bruscella, Appia-Ayme, Levican, Ratouchniak, Holmes, Jedlicki and Bonnefoy, manuscript in preparation), was highly expressed (Table 1 and Fig. 3) in agreement with Northern hybridization and real time PCR experiments ([31], Bruscella, Appia-Ayme, Levican, Ratouchniak Holmes, Jedlicki and Bonnefoy, manuscript in preparation).

The *rus* operon, encoding electron transfer proteins involved in the respiratory chain between FeII and oxygen [9], was shown by a number of approaches to be more expressed in FeII than in S^0 conditions in the strains ATCC 33020 [10,13,32,33] ATCC 19859 [22,34], or Torma [35], except in NASF-1 strain where the transcriptional level of *coxB* was similar in both conditions [23]. The spots corresponding to the genes of this operon were saturated in iron so expression ratios could not be determined. However, differential expression in iron is in agreement with previous results. Optimized image acquisition and data analysis conditions will have to be found for this case.

Surprisingly, while higher sulfide quinone reductase activity was observed in S^0 than in FeII conditions [22], two out of the three putative operons encoding sulfide

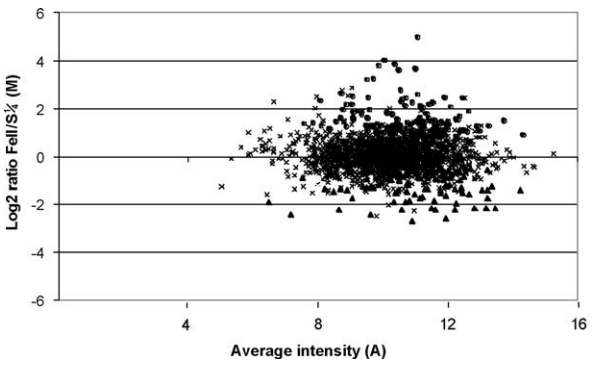

	P value	*B*-statistic
Up-regulated genes	< 0,01	> 0
Total	265	211
FeII	145	120
S¼	120	91

Fig. 2. Upregulated genes in *A. ferrooxidans* cells grown in FeII or S^0. Statistical significance was assessed by either *t*-test probability value *P* or Bayes *B*-statistic. In the left panel, circles: induced in FeII; triangles: induced in S^0.

Table 1
Microarray expression ratios between FeII and S^0 grown cells

Gene name	Gene function	*M* value	*P* value	Expression
rus operon				
cyc2	Outer membrane cytochrome *c* precursor	Saturated		
cyc1	Cytochrome c_{552} diheme precursor	Saturated		
coxB	aa_3 Cytochrome *c* oxidase II	Saturated		
coxA	aa_3 Cytochrome *c* oxidase I	Saturated		
coxC	aa_3 Cytochrome *c* oxidase III	Saturated		
rus	Rusticyanin	Saturated		
rus	Rusticyanin	Saturated		
rus	Rusticyanin	Saturated		
cydAB encoding bd ubiquinol oxidase				
cydA	Cytochrome *d* ubiquinol oxidase I (*bd*)	−0.75	0.128	ND
cydB	Cytochrome *d* ubiquinol oxidase II (*bd*)	−1.22	0.065	ND
cyoBACD encoding bo_3 *ubiquinol oxidase*				
cyoB	Cytochrome *o* ubiquinol oxidase subunit II	**−1.97**	**0.008**	**NL**
cyoA	Cytochrome *o* ubiquinol oxidase subunit I	**−2.69**	**0.008**	**NL**
cyoC	Cytochrome *o* ubiquinol oxidase subunit III	**−2.49**	0.020	ND
cyoD	Cytochrome *o* ubiquinol oxidase subunit IV	−1.45	0.113	ND
doxI operon encoding thiosulfate quinol reductase				
doxDA1	thiosulfate quinol oxido-reductase	1.49	0.056	ND
doxII operon encoding thiosulfate quinol reductase				
doxDA2	thiosulfate quinol oxido-reductase	−1.41	0.029	ND
rod	Rhodanese-related sulfurtransferase	−0.95	0.061	ND
petI operon				
cycA1	Cytochrome *c*4 precursor (*c*-552)	**3.61**	**0.000**	***DF***
petA1	Ubiquinol-cytochrome *c* reductase, Rieske protein	**3.47**	**0.000**	***DF***
petB1	Ubiquinol-cytochrome *c* reductase, cytochrome *b*	**5.25**	**0.001**	***DF***
petC1	Ubiquinol-cytochrome *c* reductase, cytochrome *c*1	**3.41**	**0.000**	***DF***
petII operon				
cycA2	Cytochrome *c*4 precursor (*c*-552)	−0.40	0.192	ND
petA2	Ubiquinol-cytochrome *c* reductase, Rieske protein	−1.35	**0.012**	**NL**
petB2	Ubiquinol-cytochrome *c* reductase, cytochrome *b*	−1.42	**0.013**	**NL**
petC2	Ubiquinol-cytochrome *c* reductase, cytochrome *c*1	0.09	0.780	ND
hip	High redox potential iron–sulfur protein (HiPIP)	−1.04	0.031	ND
sqrI operon encoding sulfide quinone reductase				
sqrI	Sulfide quinone reductase	**2.16**	**0.000**	***DF***
sqrII operon encoding sulfide quinone reductase				
sqrII	Sulfide quinone reductase	**2.47**	**0.000**	***DF***
sqr3 gene encoding sulfide quinone reductase				
sqr3	Sulfide quinone reductase	0.59	0.491	ND

ND: not differential ($P>0.01$), NL: near cut-off limit: (are significant according to one of the test criteria, e.g. $P\leq0.01$, therefore indefinite). In **bold**: $P\leq0.01$. ***DF***: Differential FeII up ($P<0.01$ and $M>0$).

quinone reductase (*sqrI* and *II*) showed a 5 fold higher expression ($M=2.17\pm0.63$) in FeII- than in S^0-grown cells (Table 1). However, these two operons are constituted of paralogue genes: *sqr* and three other genes encoding hypothetical proteins. Likely, the identity level of these genes prevented the differentiation of their expression levels by microarrays using 50-mers oligonucleotides. The third *sqr* gene (*sqr3*), included in a different gene context, does not seem to be differentially expressed in either conditions, contrary to what was observed in *A. ferrooxidans* NASF-1, where the transcriptional level of *sqr3* was found to be three fold higher in S^0 than in FeII-grown cells [23]. Further experiments are therefore required to explain these discrepancies.

3.2.2. Characterization of S^0-induced genes encoding electron transporters

Several genes of the *cyd*, *cyo*, *doxII* and *petII* operons presented differences in expression that were very near the statistic significance cut-off limit established in the present analysis (Table 1) and were thus considered as differentially expressed. Therefore, these operons seem to be more expressed in S^0 than in FeII conditions, in agreement with previous results. We have indeed shown by Northern hybridization and real time PCR that the *petII* operon is slightly expressed in S^0 than in FeII conditions in the ATCC 33020 strain ([31], Bruscella, Appia-Ayme, Levican, Ratouchniak, Holmes, Jedlicki and Bonnefoy, manuscript in

preparation). The same holds true for the *rod* gene encoding a rhodanese-like proteins [20] and belonging to the putative *doxII* operon. Furthermore, higher amounts of quinol oxidases and higher activities of quinol oxidases and thiosulfate quinol reductase have been observed in ATCC 19859 cells grown in S^0 compared to those grown in FeII [22]. However, in the NASF-1 strain, the transcription of the *cydA* gene encoding subunit I of the alternate *bd* quinol oxidase was similar in both conditions [23].

Table 2
Comparison of raw fold changes in gene expression between FeII- and S^0-grown cells (midlog) obtained by microarray analysis and real time PCR (*) in this work

Upregulated in Fe or in S^0	Gene expression ratios		
	Microarray	Real-time PCR	
	Fold (*)	Fold change (*)	Fold change
cyc2	4.6[c]		4.9[a]
cyc1	11.6[c]		23.5[a]
orf	8.4[c]		8.85[a]
coxB	9.6[c]		17.5[a]
coxA	–		9.46[a]
coxC	4.4[c]		5.68[a]
rus	5.8[c]		24.5[a]
cycA1	13.0		47.4[b]
sdrA1	20.3	22.5	55.8[b]
petA1	12.0		145.12[b]
petB1	27.6		65.77[b]
petC1	11.6		60.67[b]
cycA2	0.2		4.65[b]
sdrA2	0.8		0.88[b]
petA2	1.8		2.77[b]
petB2	2.0		3.73[b]
petC2	–		1.48[b]
hip (iro)	1.1		8.05[b]
Gene downstream from *sqr2*	5.2	4.8	10.53
cyoA	7.2	6	12.45
cydA	0.6	1.7	4.43
Gene upstream from *doxDA2*	2.6	3	6.74
rod (downstream from *doxDA2*)	0.9		2.39
Not differentially expressed	Fold	Fold	Fold
Gene downstream from *sqr1*	1.2	2.1	1.97
sqr3	0.3	1.5	1.01
Gene upstream from *doxDA1*	0.2	1.4	1.17

Underlined: higher expression in FeII; dotted underlined: higher expression in S^0. Real-time PCR data from [a]: [10,32,33]; [b]: ([31], Bruscella, Appia-Ayme, Levican, Ratouchniak, Holmes, Jedlicki and Bonnefoy, manuscript in preparation); [c]: [data obtained from unsaturated spots].

3.3. Validation of microarrays results using real-time PCR

To confirm the expression patterns observed with the microarrays, some genes were selected for further analysis by real-time PCR. The *rrs* gene coding for the 16S rRNA has been shown to be expressed at the same (constitutive) level under both conditions of growth (FeII- and S^0-medium) [10] and was used as the reference standard. Raw fold changes in expression are shown in Table 2. The expression ratios obtained by real-time-PCR of most of these genes correlated well with those obtained with microarrays (Table 2). However, as described previously in other cases, the transcript levels values obtained by real-time PCR were higher than with the microarrays, in accordance with the higher sensitivity of the former technique. Despite of these (minor) quantitative differences, the results obtained by real-time PCR were in good agreement with those obtained from microarrays and support the general consistency between the two methods for measuring relative expression levels.

To differentiate the expression of the two identical *sqrI* and *sqrII* operons, 20-mers oligonucleotides were designed in the very beginning or very end of the gene clusters where the sequences differ. Real-time PCR with these oligonucleotides indicated that *sqrII* is 10.53 fold more expressed in FeII than in S^0 conditions, while *sqrI* is almost evenly expressed in both conditions (Table 2). Thus, differential regulation of paralogue genes which sequences are highly similar could be distinguished by real-time PCR with adequate designed oligonucleotides.

For the genes of the *petII, cyd, cyo* and *doxII* operons where *B* and/or *P* values were near the cut-off limit, real-time PCR experiments clearly showed higher expression in S^0 than in FeII conditions (Table 2).

In the case of the *rus* operon, which corresponding spots were saturated on microarrays, higher expression in FeII- than in S^0-grown cells was obtained by real-time PCR [10,32,36] (Table 2).

4. Conclusion

Global changes in transcript abundance, reflecting the primary response of *A. ferrooxidans* to energy source changes are in agreement with previous findings for most genes. The differential expression of the *rus, petI*, *petII*, *cyd*, *cyo*, *doxII* operons encoding electron transfer proteins, is consistent with existing data ([9,10,20,22,31–33,36], Bruscella, Appia-Ayme, Levican, Ratouchniak, Holmes, Jedlicki and Bonnefoy, manuscript in preparation). Combined microarrays and

real-time PCR data supported the FeII and S^0 respiratory chain model we have proposed (Fig. 3) ([9,22,23,29–31,33], Bruscella, Appia-Ayme, Levican, Ratouchniak, Holmes, Jedlicki and Bonnefoy, manuscript in preparation). In this model, the outer membrane cytochrome *c*, Cyc2, transfers electrons from FeII to the periplasmic rusticyanin, which passes them to the membrane-bound cytochrome c_4, Cyc1, and from there to the cytochrome oxidase CoxBACD where oxygen is reduced to water. All these redox proteins are encoded by the *rus* operon [9]. FeII oxidation and NAD(P) reduction has been proposed to be coupled to explain the balance of the electron flow from FeII between two pathways: the exergonic one, through the aa_3 type oxidase towards oxygen encoded by the *rus* operon, and the endergonic one, through a bc_1 complex toward NAD(P) [24,37]. In the reverse electron (endergonic) pathway the bc_1 complex receives electrons from a cytochrome *c* and transfers them to the quinol pool. We have proposed that this bc_1 complex and this

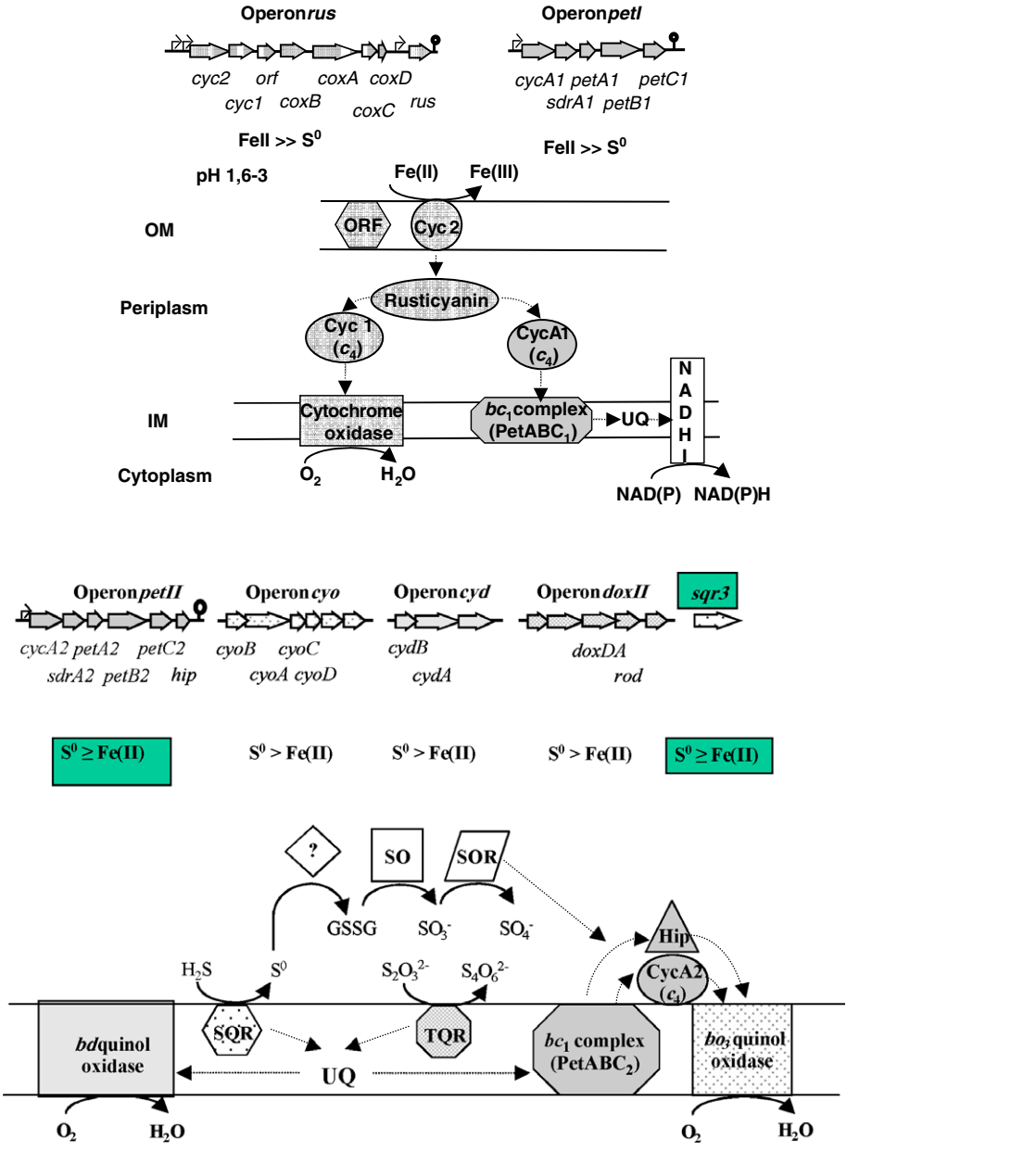

Fig. 3. Model proposed for iron and sulfur energetic metabolism of *A. ferrooxidans*. The transcriptional units and the corresponding redox proteins are presented in the same color. TQR: thiosulfate quinol reductase; SQR: sulfide quinone reductase; Hip: High Potential Iron–sulfur protein.

cytochrome *c* are encoded by the *petI* operon ([30,31], Bruscella, Appia-Ayme, Levican, Ratouchniak, Holmes, Jedlicki and Bonnefoy, manuscript in preparation) and that the rusticyanin can give electrons to two different cytochromes c_4: CycA1 encoded by the *petI* operon or Cyc1 encoded by the *rus* operon ([31], Bruscella, Appia-Ayme, Levican, Ratouchniak, Holmes, Jedlicki and Bonnefoy, manuscript in preparation). In the former case, electrons are transferred to the endergonic pathway to oxygen while in the later case, they are transferred to the exergonic pathway to NAD(P). In *A. ferrooxidans*, the cytochrome bc_1 complex has been shown to function in reverse in FeII grown cells, even in the presence of thiosulfate, while it functions in the forward direction in S^0 grown cells [22,24]. According to our model, the bc_1 complex encoded by *petI* is the one functioning in reverse and transfers the electrons from ferrous iron to NAD(P), while the bc_1 complex encoded by *petII* is the one functioning in the forward direction and transfers electrons from sulfur to oxygen ([31], Bruscella, Appia-Ayme, Levican, Ratouchniak, Holmes, Jedlicki and Bonnefoy, manuscript in preparation). When functioning in the forward direction, the bc_1 complex receives electrons from the quinol pool and transfers them either to a membrane-bound cytochrome *c*, and/or to a soluble redox protein such a cytochrome *c*, or a high potential iron–sulfur protein (HiPIP) which then gives the electron to the terminal oxidase where oxygen reduction takes place [38–40]. Since a membrane-bound cytochrome *c* (CycA2) and a soluble HiPIP are encoded by the *petII* operon, we have suggested that these two redox proteins transfer electrons between the two integral membrane complexes: the bc_1 and the terminal oxidase ([31], Bruscella, Appia-Ayme, Levican, Ratouchniak, Holmes, Jedlicki and Bonnefoy, manuscript in preparation).

We propose to continue our microarray investigations, not only providing a deeper analysis of the existing comparison between transcription in FeII versus S^0 grown cells but also extending the work to investigate transcription in cells grown in different concentrations of FeII and at different pHs. Pertinent aspects of our working models derived from the combination of bioinformatic and microarray analysis will be subjected to confirmation by real-time PCR and, where feasible, by mutant construction and analysis, genetic complementation and biochemical experiments.

Acknowledgements

Work supported in part by Fondecyt 1010623 and 1050063, Conicyt/CNRS, “Geomex” and “Puces à ADN” from the Centre National de la Recherche Scientifique and NSF. RQ was the recipient of an American Society for Microbiology Antorcha Fellowship and was supported by scholarships from the DAAD and from the Fundación Ciencia para la Vida, Chile. CAA was supported by a CNRS post-doctoral fellowship. We thank the Institute vfor Genome Research (TIGR) for the use of their genome sequence of *A. ferrooxidans*.

References

[1] Baker, B.J., Banfield, J.F., FEMS Microbiol. Ecol., 44 (2003), 139–152.
[2] Johnson, D.B., Hallberg, K.B., Res. Microbiol., 154 (2003), 466–473.
[3] Schippers, A., Sand, W., Appl. Environ. Microbiol., 65 (1999), 319–321.
[4] Yamanaka, T., et al., in: Mukohata, Y. (Ed.), New Era of Bioenergetics, Academic Press, Tokyo, 1991, pp. 223–246.
[5] Bruschi, M., Cavazza, C., Giudici-Orticoni, M.T., Déchets, 4 (1996), 27–30.
[6] Blake, R.C., Shute, E.A., Biochemistry, 33 (1994), 9220–9228.
[7] Ingledew, W.J., Cox, J.C., Halling, P.J., FEMS Microbiol. Lett., 2 (1977), 193–197.
[8] Giudici-Orticoni, M.T., et al., Biochemistry, 39 (2002), 7205–7211.
[9] Appia-Ayme, C., et al., Appl. Environ. Microbiol., 65 (1999), 4781–4787.
[10] Yarzabal, A., et al., Microbiology, 150 (2004), 2113–2123.
[11] Appia-Ayme, C., et al., FEMS Microbiol. Lett., 167 (1998), 171–177.
[12] Giudici-Orticoni, M.T., et al., J. Biol. Chem., 274 (1999), 30365–30369.
[13] Yarzabal, A., Brasseur, G., Bonnefoy, V., FEMS Microbiol. Lett., 209 (2002), 189–195.
[14] Yarzabal, A., et al., J. Bacteriol., 184 (2002), 313–317.
[15] Tabita, R., Silver, M., Lundgren, D.G., Can. J. Biochem., 47 (1969), 1141–1145.
[16] Sugio, T., et al., Appl. Environ. Microbiol., 54 (1988), 153–157.
[17] Sugio, T., et al., J. Bacteriol., 169 (1987), 4916–4922.
[18] Silver, M., Lundgren, D.G., Can. J. Biochem., 46 (1968), 1215–1220.
[19] Silver, M., Lundgren, D.G., Can. J. Biochem., 46 (1968), 457–461.
[20] Ramirez, P., et al., Appl. Environ. Microbiol., 68 (2002), 1837–1845.
[21] Kuenen, J.G., et al., in: Torma, A.E., Apel, M.L., Brierley, C.L. (Eds.), Biohydrometallurgical Technologies, vol. 2, TMS, Warrendale, PA, 1993, pp. 487–494.
[22] Brasseur, G., et al., Biochim. Biophys. Acta, 1656 (2004), 114–126.
[23] Wakai, S., Kikumoto, M., Kanao, T., Kamimura, K., Biosci. Biotechnol. Biochem., 68 (2004), 2519–2528.
[24] Brasseur, G., et al., Biochim. Biophys. Acta, 1555 (2002), 37–43.
[25] Liu, Z., et al., J. Bacteriol., 182 (2000), 2269–2276.
[26] Liu, Z., Borne, F., Ratouchniak, J., Bonnefoy, V., Hydrometallurgy, 59 (2001), 339–345.
[27] Kane, M.D., Jatkoe, T.A., Stumpf, C.R., Lu, J., Thomas, J.D., Madore, S.J., Nucleic Acids Res., 28 (2000), 4552–4557.
[28] Aiba, H., Adhya, S., de Crombrugghe, B., J. Biol. Chem., 256 (1981), 11905–11910.

[29] Smyth, G.H., Stat. Appl. Genet. Mol. Biol., 3 (2004), 3.
[30] Levican, G., et al., J. Bacteriol., 184 (2002), 1498–1501.
[31] Bruscella, P., Etude des opérons petI et petII codant pour deux complexes bc1 chez la bactérie acidophile chimioautotrophe stricte *Acidithiobacillus ferrooxidans*, PhD Thesis, Université de la Méditerranée, Aix-Marseille II, 2004.
[32] Yarzabal, A., Duquesne, K., Bonnefoy, V., in: Ciminelli, V.S.T., et Garcia, Jr., O. (Eds.), Biohydrometallurgy: Fundamentals, Technology and Sustainable Development, Elsevier, Amsterdam, 2001, pp. 253–261.
[33] Yarzabal, A., Etude de l'opéron rus, codant pour sept protéines transporteurs d'électrons, chez la bactérie acidophile, chimioautotrophe obligatoire, *Acidithiobacillus ferrooxidans*, PhD Thesis, Université de la Méditerranée, Aix-Marseille II, 2003.
[34] Pulgar, V., et al., in: Torma, A.E., Apel, M.L., Brierley, C.L. (Eds.), Biohydrometallurgical Technologies. The Minerals, vol. 2, Metals and Material Society, Warrendale, PA, 1993, pp. 541–548.
[35] Jedlicki, E., et al., Biotechnol. Appl. Biochem., 8 (1986), 342–350.
[36] Yarzabal, A., Duquesne, K., Bonnefoy, V., Hydrometallurgy, 71 (2003), 107–114.
[37] Elbehti, A., Brasseur, G., Lemesle-Meunier, D., J. Bacteriol., 182 (2000), 3602–3606.
[38] Trumpower, B.L., Microbiol. Rev., 54 (1990), 101–109.
[39] Bonora, P., et al., Biochim. Biophys. Acta, 1410 (1999), 51–60.
[40] Pereira, M.M., Carita, J.N., Teixeira, M., Biochemistry, 38 (1999), 1268–1275.